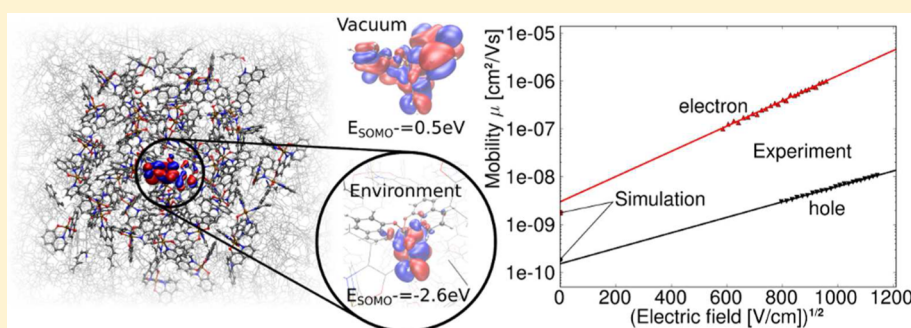


Ab Initio Treatment of Disorder Effects in Amorphous Organic Materials: Toward Parameter Free Materials Simulation

Pascal Friederich, Franz Symalla, Velimir Meded, Tobias Neumann, and Wolfgang Wenzel*

Institute of Nanotechnology (INT), Karlsruhe Institute of Technology (KIT), Karlsruhe 76021, Germany

S Supporting Information



ABSTRACT: Disordered organic materials have a wide range of interesting applications, such as organic light emitting diodes, organic photovoltaics, and thin film electronics. To model electronic transport through such materials it is essential to describe the energy distribution of the available electronic states of the carriers in the material. Here, we present a self-consistent, linear-scaling first-principles approach to model environmental effects on the electronic properties of disordered molecular systems. We apply our parameter free approach to calculate the energy disorder distribution of localized charge states in a full polaron model for two widely used benchmark-systems (tris(8-hydroxyquinolino)aluminum (Alq_3) and N,N' -bis(1-naphthyl)- N,N' -diphenyl-1,1'-biphenyl-4,4'-diamine (α -NPD)) and accurately reproduce the experimental charge carrier mobility over a range of 4 orders of magnitude. The method can be generalized to determine electronic and optical properties of more complex systems, e.g. guest–host morphologies, organic–organic interfaces, and thus offers the potential to significantly contribute to de novo materials design.

Organic materials are key constituents of a wide range of low-cost, technologically relevant materials, readily utilized in such devices as organic light emitting diodes (OLEDs),^{1,2} organic photovoltaics (OPV),^{3–5} and organic field effect transistors.⁶ In the past few years, substantial strides were made resulting in an increase of the device efficiency^{7–10} as well as improvements of the manufacturing methods e.g. solvent processing, large scale printing of organic components, etc.^{11,12} There is nearly an infinite variety of different organic materials - both small molecules and polymers - which can be used pure or in different mixtures and/or as multilayer structures. Therefore, optimization in the form of experimental fabrication, small scale production, and characterization of samples for material screening remains a costly challenge to experimentalists. Predictive analytical and computational modeling of candidate materials may greatly reduce cost and accelerate the design of new materials. Bottom up modeling further elucidates the physical processes in the device and may consequently offer great help in systematic material design. The intrinsic difficulty in modeling amorphous organic materials is 2-fold. While the disorder of the system requires the handling of sizable samples to converge statistics, the quantum mechanical nature of the relevant physics for charge transport and light-matter interactions requires quantum mechanical calculations. For

charge transport processes, the situation is further aggravated as polarization effects of moving charges are dynamic properties. In materials of weakly coupled molecules in particular, the electrostatic polarization of the surrounding molecules creates the individual electronic properties of each molecule.

State-of-the-art calculations^{13–17} are either parametrized semiclassical polarizable force-field approaches^{18–21} (PFF), QMMM methods,^{14,22,23} or quantum-mechanical constrained DFT^{24–27} approaches (cDFT). In the PFF and QMMM case, the charge density of the environment is mapped to polarizable point charges which are included in single molecule calculations. In that case, nonadiabatic polarization effects on the wave functions are neglected. cDFT, on the other hand, is fully quantum mechanical and uses artificial potentials to confine the charge carriers to certain molecules in the system but requires computationally very demanding QM calculations for large systems, creating a challenge on statistical convergence. To overcome the bottleneck on both ends, we present here a linearly scaling, first-principles quantum mechanical method (quantum patch approach) to model polarization effects in amorphous materials which we apply to

Received: May 14, 2014

Published: July 16, 2014

calculate charge hopping rates in the two commonly used benchmark systems tris(8-hydroxyquinolino) aluminum (Alq_3) and N,N' -bis(1-naphthyl)- N,N' -diphenyl-1,1'-biphenyl-4,4'-diamine (α -NPD).

When modeling charge transport in disordered organic materials, where charges propagate by a succession of leaping processes between neighboring localized sites, the hopping transport formalism is a common starting point. When the sites are weakly coupled²⁸ and the time scale of local charge reorganization is smaller than the time scale of a single hopping processes, Marcus theory²⁹ is widely used for the calculation of charge hopping rates

$$k_{\text{if}} = \frac{2\pi}{\hbar} |J_{\text{if}}|^2 \frac{1}{\sqrt{4\pi\lambda_{\text{if}}k_{\text{B}}T}} \exp\left(-\frac{(\lambda_{\text{if}} + \Delta G_{\text{if}})^2}{4\lambda_{\text{if}}k_{\text{B}}T}\right) \quad (1)$$

where k_{if} is the hopping rate, \hbar is the Plank constant, J_{if} is the electronic coupling, λ_{if} is the reorganization energy, k_{B} is the Boltzmann factor, ΔG_{if} is the Gibbs free energy difference of the initial and final state. The Marcus rate depends on three microscopic quantum-mechanical parameters - J_{if} , ΔG_{if} and λ_{if} . The state energy difference resulting from different environments of the two hopping sites is strongly dependent on the local details of the structure of the system. Materials specific parameters can be mapped onto transport models, which can then be used for the calculation of charge carrier mobility and other experimentally relevant quantities in master equation approaches.^{30–32}

The resulting mobility is highly sensitive to changes of the width of the density of states or the energy disorder $\sigma(E)$, as it enters the functional form in the exponent in quadratic fashion ($\mu \propto \exp(-C(\sigma/(k_{\text{B}}T))^2)$).^{33–36} C is a factor dependent on spatial correlations in the system which depends on the details of the model and ranges from $C \approx 1/4$ in effective medium models³⁷ to $C \approx 1/2$ ³⁸ for short-range lattice models with uncorrelated disorder. The energy disorder σ is defined as the width of the local on-site energy distribution of the system, having its origin in disorder on the local electronic states induced by the amorphous nature of the materials. Hence, an accurate description of the local electronic structure underlying the processes on the molecular length-scale is of great importance. Feeding the respective microscopic parameters obtained with the quantum patch approach in the appropriate master equation approach accurately reproduces experimental electron and hole mobilities for Alq_3 and hole mobilities for α -NPD (no experimental data for electrons available).

COMPUTATIONAL APPROACH

In the quantum patch approach, the Hamilton operator for a system of N weakly coupled molecules with the total density $n(\mathbf{r})$ is approximated by

$$\hat{H} = \text{diag}(H_1[n_{\text{tot}}(\vec{r})], \dots, H_N[n_{\text{tot}}(\vec{r})]) \quad (2)$$

neglecting intermolecular contributions to kinetic energy and exchange interactions, an approximation made in many embedding methods for weakly coupled molecules.^{16,18,39}

With this approximation, the Hamiltonian for each molecule can be solved separately for each of the molecules as long as the total charge density is known. To iteratively solve the electronic structure of the system we partition the total charge density $n_{\text{tot}}(\mathbf{r})$ into a sum of charge densities of the single molecules. In the calculation of molecule i , the charge densities $n_{j \neq i}(\mathbf{r})$ of the

other molecules are replaced by a set of point charges where k is the index of the respective atom at position $\mathbf{R}_{j,k}$.

$$n_{\text{tot}}^{\mu}(\vec{r}) = n_i^{\mu}(\vec{r}) + \sum_{j \neq i, k} q_{j,k}^{\mu} \delta(\vec{r} - \vec{R}_{j,k}) \quad (3)$$

Intermolecular electrostatic interactions are taken into account by employing partial charges fitted with the Merz–Singh–Kollman scheme (ESP-charges)⁴⁰ which are specifically designed to approximately reproduce the electrostatic field of a molecule. These charges are therefore well suited to reproduce the electrostatic environment required for the treatment of polarization effects. We begin by guessing initial partial charges $q_{j,k}^0$, using vacuum partial charges for each molecule, and then solve the Schrödinger equation for each molecule self-consistently. We update the partial charges of the current molecule on the basis of the new electron densities $n_i^{\mu}(\mathbf{r}) = \sum_j |\Phi_{ij}^{\mu}(\mathbf{r})|^2$ for molecule i with Kohn–Sham orbitals

Φ_{ij}^{μ} . These densities will be used in the subsequent calculations for the other molecules, such that μ denotes the iteration step. As indicated in Figure 1 we iterate this procedure for all

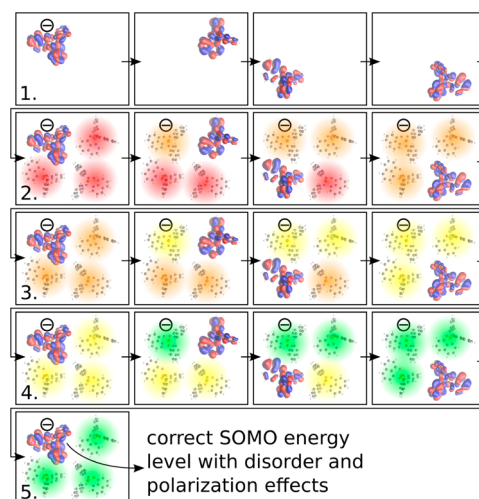


Figure 1. Schematic description of the algorithm used for the calculation of energy disorder. In the first step, vacuum partial charges for each molecule are calculated. Afterward, an additional charge is assigned to a certain molecule. Partial charges of this as well as of the neighboring molecules within a certain cutoff distance are self-consistently re-evaluated using a cloud of point charges that are iteratively improved until convergence in total energy of the charged molecule is reached. This procedure is repeated for positive and negative additional charges on each molecule in the system.

molecules in the system of interest until convergence (see the SI). For practical reasons, we do all calculations of one iteration step in parallel and update the partial charge environment for each molecule afterward in the next iteration step.

In order to calculate the hopping rates of electrons (holes) as described in eq 1, the Gibbs free energy difference ΔG_{if} of negatively (positively) charged hopping sites is needed as input. In the absence of external fields and entropic effects, ΔG_{if} is generally approximated by the total energy difference ΔE_{if} between the final and the initial state.^{18,41} Besides vibrational effects, the unique shape and environment of each molecule in the system determines these energy differences. Therefore, they are calculated for each pair of hopping sites with the method outlined above, using an environment of self-consistent point

charges surrounding the single monomers. In order to describe polaron effects an additional charge is assigned to molecule i , and its vacuum partial charges are calculated and the total energy of the system is self-consistently calculated. Formally, this approach is an approximation of the frozen density embedding method^{42–44} including polarization effects due to explicit additional charges in the system. One now has to repeat this procedure by putting an additional charge on the target molecule f of the hopping process. The result is the energy E_i^- (E_i^+), from which we compute the energy differences for electron (hole) transport $\Delta E_{\text{electron}}$ (ΔE_{hole}). Averaging these energy differences over samples of sufficient size, the energy disorder distribution $\sigma(\Delta E) = (1/(N_{\text{pairs}} - 1) \sum \Delta E^2)^{1/2}$ is

computed for all nearest-neighboring pairs in the morphology. It should be remarked that these σ reflect the local disorder and only match the global energy disorder in case of no energy correlation between neighboring molecules.

To estimate charge carrier mobilities we employ the analytic solution of the master equation for Marcus rates in a homogeneous medium by Rodin et al. (unpublished work)

$$\mu = \mu_0 \exp\left[-\frac{1}{4}(\beta\sigma)^2\right] \quad (4)$$

with

$$\mu_0 = \frac{e\beta M \langle J^2 r^2 \rangle}{n\hbar\sqrt{\lambda}} \sqrt{\frac{\pi\beta}{1 + \frac{\beta\sigma^2}{\lambda}}} \exp\left[-\frac{1}{4}\beta\lambda\right] \quad (5)$$

Consistently with our microscopic energy disorder, Rodin et al. use a local disorder parameter $\sigma(E)$, which inherently includes energy correlations and show their thusly modified effective medium approach to work well for materials with both strong and weak disorder. $\beta = 1/k_B T$ is the inverse temperature, n is the dimension, and M is the mean number of nearest neighbor molecules. We calculated the electronic coupling constants with a Löwdin orthogonalization method⁴⁵ using dimer Fock- and overlap matrices and frontier orbitals of uncharged monomers within a self-consistently evaluated point charge environment. The inner part of the reorganization energy was calculated in geometry optimizations of charged molecules starting from the optimized geometry of the neutral molecule and vice versa.

RESULTS AND DISCUSSION

To validate this approach we investigate widely studied meridional tris(8-hydroxyquinolino)aluminum (Alq_3) and N,N' -bis(1-naphthyl)- N,N' -diphenyl-1,1'-biphenyl-4,4'-diamine (α -NPD).^{46,47} Alq_3 has a selective charge carrier mobility, conducting electrons much better than holes and a large molecular dipole moment, which leads to strong environment effects and large energy disorder. α -NPD, on the other hand, is a widely used hole transport material with comparatively low disorder and consequently high charge carrier mobility. For Alq_3 , a morphology generated with the VOTCA^{16,48} package was used. It contains 512 molecules and was periodically extended in each direction in order to reach convergence for long-range electrostatic interaction. The α -NPD morphology comprising 300 molecules was generated with a molecular dynamics protocol similar to that used in GROMACS⁴⁹ (see the SI) and also extended periodically. All quantum mechanical DFT calculations were performed with the quantum chemistry

package TURBOMOLE.⁵⁰ If not indicated otherwise, all DFT calculations were performed with the B3-LYP⁵¹ functional and the def2-SV(P)⁵² basis sets. We find that typically 7 iteration steps for the self-consistent treatment of polarization effects as explained in Figure 1 and 100 neighboring molecules for each charged hopping center are required to reach convergence.

Figure 2 shows distributions of site energy differences in an Alq_3 system. In order to demonstrate the influence of the

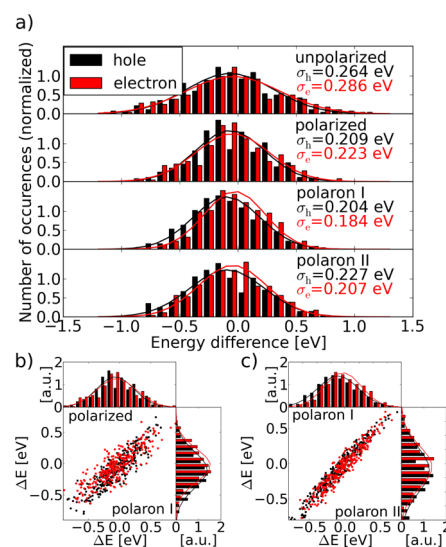


Figure 2. Distribution of site energy differences in an Alq_3 morphology. In a) we show all four different approaches to calculating $\sigma(E)$ (see text). The unpolarized approach shows both electron and hole distributions being very wide with electrons being wider, which should lead to hole mobility being larger than electron mobility. The most precise polaron II approach shows narrower distributions with the electron σ being smaller than the hole $\sigma(E)$. b) Polarized vs Polaron I calculation: the order of energy disorder strength for electrons and holes interchanges and the scatter plot is very wide indicating very different local results. c) Polaron I vs Polaron II: The narrow distribution of points in the scatter plot indicates that it is most important to treat the system on a quantum mechanical level. The choice of orbital energies vs total energies has a much smaller effect.

environmental disorder effect we report results for the “unpolarized” model, neglecting environmental polarization effects altogether, the “polarized” model which computes site energy differences of neutral molecules in the presence of environmental polarization and the “polaron” model, which computes site energy differences of charged molecules in the presence of environmental polarization. For the polaron model we distinguish model I, which uses orbital energies as the other models and model II, which uses total energies of charged ($E_{\text{tot},i/f}^{\pm}$) and uncharged ($E_{\text{tot},i/f}^0$) molecules as in

$$\Delta E_{e/h} = (E_{\text{tot},f}^{-/+} - E_{\text{tot},f}^0) - (E_{\text{tot},i}^{-/+} - E_{\text{tot},i}^0) \quad (6)$$

where i and f indicate the indices of the molecules participating in the hopping process. In the unpolarized case, the molecules are embedded into a point charge environment consisting of ESP charges derived in DFT calculations of single molecules in vacuum. As shown in Figure 2, the width of the energy disorder distribution $\sigma(E)$ decreases by 21% from 0.264 to 0.209 eV for holes and 22% from 0.286 to 0.223 eV for electrons stemming from the explicit polarization of the environment. The anticipated order of energy disorder for electrons and holes is still not captured. Models using an effective or distance

depending dielectric constant can capture this effect in principle,¹⁶ but these models are typically valid for distances considerably larger than molecular diameters. For small distances, there are difficulties¹⁶ to use an effective screening constant $\epsilon(r)$ that arise from the local influence of orbital shapes, sizes, and polarizabilities. In Figure 3 the shape of the

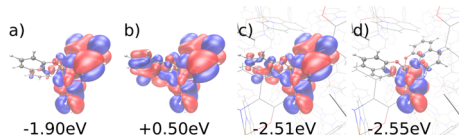


Figure 3. Comparison between LUMO orbitals (a,c) of a selected uncharged Alq_3 molecule and SOMO^- orbitals (b,d) of additional electrons without (a,b) and with (c,d) converged self-consistently evaluated point charge environment. The treatment of explicit charges as well as the explicit electrostatic environment changes the shapes and energies of the respective orbitals significantly. The orbital energies directly feed-back into the site-energy differences and thereby energy disorder.

unpopulated lowest unoccupied molecular orbital (LUMO) orbital of a monomer without and with polarized environment is compared to the shape of the populated single occupied molecular orbital (SOMO^-) orbital of the same monomer for one sample molecule. Equilibration of the environment leads to a stabilization of the respective orbital energy. Both LUMO and SOMO^- have similar energies in environment, whereas their shape and consequently polarizability are clearly different, showing that the consideration of explicit additional charge leads to different orbital structures and thus different interaction with the local environment.

The comparison between the energy disorder in an Alq_3 and an $\alpha\text{-NPD}$ system is shown in Table 1. The large difference in

Table 1. Energy Disorder Comparison for Both Electron and Hole Transport Obtained with Four Different Methods^a

energy disorder [eV]		unpolarized	polarized	polaron I	polaron II
Alq_3	hole	0.264	0.209	0.204	0.227
	electron	0.286	0.223	0.184	0.207
$\alpha\text{-NPD}$	hole	0.148	0.144	0.149	0.153
	electron	0.114	0.107	0.092	0.099

^aPolaron I refers to use of the frontier orbital energies, while Polaron II stands for use of total energies instead.

the vacuum dipole moment (B3-LYP/def2-SV(P)) of $\alpha\text{-NPD}$ (0.31 D) compared to Alq_3 (4.40 D) leads to tremendous differences in energy disorder of these two materials. Disorder in $\alpha\text{-NPD}$ mostly arises from different geometric conformations of the molecules in the morphology rather than their individual electrostatic environment which also results in weaker polarization effect. As it is well-known within DFT, the electron density is a physical quantity, while Kohn–Sham orbitals are not, making use of total energies, which depend on the electron density physically more robust and the method more readily extendable to other ab initio approaches. Thus, we use the polaron II model for the calculation of the charge carrier mobility. However, the trend that disorder is weaker for electrons than for the holes also holds for the polaron I model.

The mean electronic coupling $\langle J^2 r^2 \rangle$ and the reorganization energy λ have been computed using the same samples and are shown in Table 2. For the electronic coupling elements, the B3-

Table 2. Parameters for Mean Electronic Coupling $\langle J^2 r^2 \rangle$ and Reorganization Energy λ ^a

		$\langle J^2 r^2 \rangle$ [eV ² Å ²]	λ [eV]
Alq_3	hole	9.05×10^{-3}	0.213
	electron	7.80×10^{-3}	0.308
$\alpha\text{-NPD}$	hole	1.33×10^{-3}	0.253
	electron	3.84×10^{-3}	0.122

^aThe values compare well to literature values.¹⁸

LYP functional and the def2-SV(P) basis-set was used. The inner part of the reorganization energy λ is calculated using the same level of theory.

Evaluation of eqs 4 and 5 with the input parameters in Table 1 and 2 leads to the charge carrier mobilities in Table 3. The mobility values follow the charge disorder trends, i.e. larger disorder results in smaller mobility and vice versa. For Alq_3 , the quantum patch method using explicitly charged systems shows preferential electron transport, which is not the case for calculations using uncharged molecules (polarized or not). Further, when total energies (polaron model II) are used, the quantitative experimental results for the charge carrier mobility are reproduced (see Figure 4). The same holds true for $\alpha\text{-NPD}$, where the experimental hole mobility is quantitatively reproduced. We predict a surprisingly large electron mobility, which is presently not experimentally accessible due to the very shallow LUMO level of $\alpha\text{-NPD}$. With work function tuning methods,^{53,54} it can potentially become exploitable in the future.

CONCLUSION

In conclusion, we showed that the self-consistent quantum-mechanical quantum patch method for the calculation of energy disorder is able to quantitatively predict charge carrier mobilities for materials such as Alq_3 and $\alpha\text{-NPD}$, which differ strongly in their physiochemical characteristics. We show that polaron effects must be explicitly taken into account to explain differences in hole and electron mobility of Alq_3 . The quantum patch method scales linearly with the number of molecules in the system and thus allows for the treatment of system sizes up to several thousand molecules. Statistical quantities such as energy disorder can therefore be evaluated to a high level of accuracy. The fact that neither fitting parameters nor constraints (as in cDFT) are needed makes the method applicable for a wide range of problems. As environmental effects are ubiquitous in many molecular materials, the electrostatic embedding method may also be used to describe environmental effects for lifetime and mobility of excitons and charge separation near interfaces.⁵⁵ The method is expected to also be useful for explicitly feeding the disorder information in the coupling matrix elements (J 's), estimating morphology specific reorganization energies, as well as charge transport in polymers.

Methods. For Alq_3 , a morphology generated with the VOTCA^{16,48} package was used. It contains 512 molecules and was periodically extended in each direction in order to reach convergence for long-range electrostatic interaction. The $\alpha\text{-NPD}$ morphology comprising 300 molecules was generated with a molecular dynamics protocol similar to that used in GROMACS⁴⁹ (see the SI) and also extended periodically. All quantum mechanical DFT calculations were performed with the quantum chemistry package TURBOMOLE.⁵⁰ If not

Table 3. Charge Carrier Mobility for Alq₃ and α -NPD Calculated by Eqs 4 and 5 with Values for Energy Disorder σ , Coming from a Number of Different Methods (See Text) and Compared to Experimental Data^{46,47}

mobility μ [cm ² /(V s)]		unpolarized	polarized	polaron I	polaron II	exp
Alq ₃	h+	1.13×10^{-13}	4.66×10^{-9}	1.09×10^{-8}	1.87×10^{-10}	1.5×10^{-10}
	e-	2.26×10^{-16}	1.06×10^{-10}	7.16×10^{-8}	1.77×10^{-9}	3.0×10^{-9}
α -NPD	h+	7.77×10^{-6}	1.27×10^{-5}	6.86×10^{-6}	4.15×10^{-6}	7.82×10^{-6}
	e-	5.64×10^{-2}	1.10×10^{-2}	4.08×10^{-2}	2.26×10^{-2}	

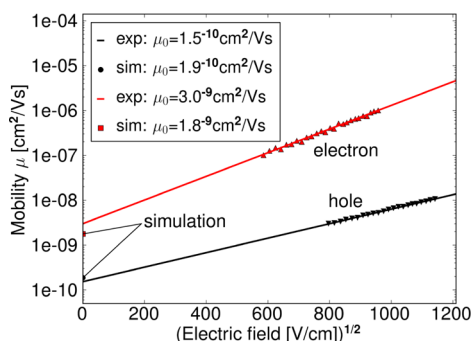


Figure 4. Comparison between experimentally measured field-dependent electron and hole mobility for Alq₃ and the simulated zero-field mobility. (Reproduced with permission from H. H. Fong and S. K. So, *J. Appl. Phys.* **100** (2006). Copyright 2006, AIP Publishing LLC.).

indicated otherwise, all DFT calculations were performed with the B3-LYP⁵¹ functional and the def2-SV(P)⁵² basis sets.

■ ASSOCIATED CONTENT

● Supporting Information

Generation of atomistic morphologies, computational details, and convergence of the quantum patch method. This material is available free of charge via the Internet at <http://pubs.acs.org>.

■ AUTHOR INFORMATION

Corresponding Author

*E-mail: wolfgang.wenzel@kit.edu.

Notes

The authors declare no competing financial interest.

■ ACKNOWLEDGMENTS

We acknowledge support by I. Kondov from SCC KIT (Germany); P. Råback and J. Pirhonen from CSC (Finland); A. Emerson from CINECA (Italy); and fruitful discussions with F. May and C. Lennartz. This work was supported by the FP-7 e-infrastructure project MMM@HPC and the PRACE6 and PRACE DEC18 projects as well as the MODEOLED project.

■ REFERENCES

- (1) Groves, C. Organic Light-Emitting Diodes: Bright Design. *Nat. Mater.* **2013**, *12*, 597–598.
- (2) Hung, L. S.; Chen, C. H. Recent Progress of Molecular Organic Electroluminescent Materials and Devices. *Mater. Sci. Eng., R* **2002**, *39*, 143–222.
- (3) Li, G.; Zhu, R.; Yang, Y. Polymer Solar Cells. *Nat. Photonics* **2012**, *6*, 153–161.
- (4) Kippelen, B.; Bredas, J.-L. Organic Photovoltaics. *Energy Environ. Sci.* **2009**, *2*, 251–261.
- (5) Hains, A. W.; Liang, Z.; Woodhouse, M. A.; Gregg, B. A. Molecular Semiconductors in Organic Photovoltaic Cells. *Chem. Rev. (Washington, DC, U. S.)* **2010**, *110*, 6689–6735.

(6) Dimitrakopoulos, C. D.; Malenfant, P. R. L. Organic Thin Film Transistors for Large Area Electronics. *Adv. Mater. (Weinheim, Ger.)* **2002**, *14*, 99–117.

(7) Green, M. A.; Emery, K.; Hishikawa, Y.; Warta, W.; Dunlop, E. D. Solar Cell Efficiency Tables (Version 39). *Prog. Photovoltaics* **2012**, *20*, 12–20.

(8) Shrestha, S. Photovoltaics Literature Survey (No. 104). *Prog. Photovoltaics* **2013**, *21*, 1429–1431.

(9) Kalyani, T.; Dhoble, S. J. Organic Light Emitting Diodes: Energy Saving Lighting Technology-a Review. *Renewable Sustainable Energy Rev.* **2012**, *16*, 2696–2723.

(10) Lezama, I. G.; Morpurgo, A. F. Progress in Organic Single-Crystal Field-Effect Transistors. *MRS Bull.* **2013**, *38*, 51–56.

(11) Hoth, C. N.; Schilinsky, P.; Choulis, S. A.; Balasubramanian, S.; Brabec, C. J., Solution-Processed Organic Photovoltaics. In *Applications of Organic and Printed Electronics*; Springer: 2013; pp 27–56.

(12) Hast, J.; Tuomikoski, M.; Suhonen, R.; Väisänen, K.-L.; Välimäki, M.; Maaninen, T.; Apilo, P.; Alastalo, A.; Maaninen, A. 18.1: Invited Paper: Roll-to-Roll Manufacturing of Printed Oleds. *SID Symp. Dig. Tech. Pap.* **2013**, *44*, 192–195.

(13) Mesta, M.; Carvelli, M.; de Vries, R. J.; van Eersel, H.; van der Holst, J. J. M.; Schober, M.; Furno, M.; Lüssem, B.; Leo, K.; Loebl, P.; Coehoorn, R.; Bobbert, P. A. Molecular-Scale Simulation of Electroluminescence in a Multilayer White Organic Light-Emitting Diode. *Nat. Mater.* **2013**, *12*, 652–658.

(14) Kwiatkowski, J. J.; Nelson, J.; Li, H.; Bredas, J. L.; Wenzel, W.; Lennartz, C. Simulating Charge Transport in Tris (8-Hydroxyquinoline) Aluminium (Alq₃). *Phys. Chem. Chem. Phys.* **2008**, *10*, 1852–1858.

(15) Lukyanov, A.; Lennartz, C.; Andrienko, D. Amorphous Films of Tris (8-Hydroxyquinolinato) Aluminium: Force-Field, Morphology, and Charge Transport. *Phys. Status Solidi A* **2009**, *206*, 2737–2742.

(16) Rühle, V.; Lukyanov, A.; May, F.; Schrader, M.; Vehoff, T.; Kirkpatrick, J.; Baumeier, B.; Andrienko, D. Microscopic Simulations of Charge Transport in Disordered Organic Semiconductors. *J. Chem. Theory Comput.* **2011**, *7*, 3335–3345.

(17) Baumeier, B.; Stenzel, O.; Poelking, C.; Andrienko, D.; Schmidt, V. Stochastic Modeling of Molecular Charge Transport Networks. *Phys. Rev. B* **2012**, *86*.

(18) Fuchs, A.; Steinbrecher, T.; Mommer, M. S.; Nagata, Y.; Elstner, M.; Lennartz, C. Molecular Origin of Differences in Hole and Electron Mobility in Amorphous Alq₃ - Multiscale Simulation Study. *Phys. Chem. Chem. Phys.* **2010**, *14*, 4259–4270.

(19) Ren, P.; Ponder, J. W. Consistent Treatment of Inter- and Intramolecular Polarization in Molecular Mechanics Calculations. *J. Comput. Chem.* **2002**, *23*, 1497–1506.

(20) Ponder, J. W.; Wu, C.; Ren, P.; Pande, V. S.; Chodera, J. D.; Schnieders, M. J.; Haque, I.; Mobley, D. L.; Lambrecht, D. S.; DiStasio, R. A., Jr; et al. Current Status of the Amoeba Polarizable Force Field. *J. Phys. Chem. B* **2010**, *114*, 2549–2564.

(21) Ponder, J. W. Tinker: Software Tools for Molecular Design. Washington University School of Medicine: Saint Louis, MO **2004**, *3*.

(22) Aqvist, J.; Warshel, A. Simulation of Enzyme Reactions Using Valence Bond Force Fields and Other Hybrid Quantum/Classical Approaches. *Chem. Rev. (Washington, DC, U. S.)* **1993**, *93*, 2523–2544.

(23) Norton, J. E.; Brédas, J.-L. Polarization Energies in Oligoacene Semiconductor Crystals. *J. Am. Chem. Soc.* **2008**, *130*, 12377–12384.

(24) Difley, S.; Wang, L.-P.; Yeganeh, S.; Yost, S. R.; Voorhis, T. V. Electronic Properties of Disordered Organic Semiconductors Via Qm/Mm Simulations. *Acc. Chem. Res.* **2010**, *43*, 995–1004.

- (25) Van Voorhis, T.; Kowalczyk, T.; Kaduk, B.; Wang, L.-P.; Cheng, C.-L.; Wu, Q. The Diabatic Picture of Electron Transfer, Reaction Barriers, and Molecular Dynamics. *Annu. Rev. Phys. Chem.* **2010**, *61*, 149–170.
- (26) Wu, Q.; Van Voorhis, T. Direct Calculation of Electron Transfer Parameters through Constrained Density Functional Theory. *J. Phys. Chem. A* **2006**, *110*, 9212–9218.
- (27) Wu, Q.; Van Voorhis, T. Direct Optimization Method to Study Constrained Systems within Density-Functional Theory. *Phys. Rev. A* **2005**, *72*, 024502.
- (28) Forrest, S. R. The Path to Ubiquitous and Low-Cost Organic Electronic Appliances on Plastic. *Nature* **2004**, *428*, 911–918.
- (29) Marcus, R. A. Chemical and Electrochemical Electron-Transfer Theory. *Annu. Rev. Phys. Chem.* **1964**, *15*, 155–196.
- (30) Čápek, V. Generalized Master Equations and Phonon-Assisted Hopping. *Phys. Rev. B* **1987**, *36*, 7442.
- (31) Čápek, V. Generalized Master Equations and Other Theories of the Phonon-Assisted Hopping Conduction. *Phys. Rev. B* **1988**, *38*, 12983.
- (32) Kasuya, T.; Koide, S. A Theory of Impurity Conduction. II. *J. Phys. Soc. Jpn.* **1958**, *13*, 1287–1297.
- (33) Bässler, H. Charge Transport in Disordered Organic Photoconductors a Monte Carlo Simulation Study. *Phys. Status Solidi B* **1993**, *175*, 15–56.
- (34) Pasveer, W. F.; Cottaar, J.; Tanase, C.; Coehoorn, R.; Bobbert, P. A.; Blom, P. W. M.; De Leeuw, D. M.; Michels, M. A. J. Unified Description of Charge-Carrier Mobilities in Disordered Semiconducting Polymers. *Phys. Rev. Lett.* **2005**, *94*, 206601.
- (35) Novikov, S. V.; Dunlap, D. H.; Kenkre, V. M.; Parris, P. E.; Vannikov, A. V. Essential Role of Correlations in Governing Charge Transport in Disordered Organic Materials. *Phys. Rev. Lett.* **1998**, *81*, 4472–4475.
- (36) Huber, D. L. Diffusion of Optical Excitation at Finite Temperatures. *J. Chem. Phys.* **1983**, *78*, 2530–2532.
- (37) Roichman, Y.; Preezant, Y.; Tessler, N. Analysis and Modeling of Organic Devices. *Phys. Status Solidi A* **2004**, *201*, 1246–1262.
- (38) Coehoorn, R.; Pasveer, W.; Bobbert, P.; Michels, M. Charge-Carrier Concentration Dependence of the Hopping Mobility in Organic Materials with Gaussian Disorder. *Phys. Rev. B* **2005**, *72*, 155206.
- (39) Nagata, Y. Polarizable Atomistic Calculation of Site Energy Disorder in Amorphous Alq3. *ChemPhysChem* **2010**, *11*, 474–479.
- (40) Singh, U. C.; Kollman, P. A. An Approach to Computing Electrostatic Charges for Molecules. *J. Comput. Chem.* **1984**, *5*, 129–145.
- (41) Marcus, R. A.; Sutin, N. Electron transfers in chemistry and biology. *Biochim. Biophys. Acta, Rev. Bioenerg.* **1985**, *811*, 265–322. Marcus, R. A. Electron Transfer Reactions in Chemistry: Theory and Experiment (Nobel Lecture). *Angew. Chem., Int. Ed. Engl.* **1993**, *32*, 1111–1121.
- (42) Wesolowski, T. A.; Warshel, A. Frozen Density Functional Approach for Ab Initio Calculations of Solvated Molecules. *J. Phys. Chem.* **1993**, *97*, 8050–8053.
- (43) Wesolowski, T. A.; Weber, J. Kohn-Sham Equations with Constrained Electron Density: An Iterative Evaluation of the Ground-State Electron Density of Interacting Molecules. *Chem. Phys. Lett.* **1996**, *248*, 71–76.
- (44) Jacob, C. R.; Neugebauer, J. Subsystem Density-Functional Theory. *Wiley Interdiscip. Rev.: Comput. Mol. Sci.* **2014**, *4*, 325–362.
- (45) Stehr, V.; Pfister, J.; Fink, R. F.; Engels, B.; Deibel, C. First-Principles Calculations of Anisotropic Charge-Carrier Mobilities in Organic Semiconductor Crystals. *Phys. Rev. B* **2011**, *83*, 155208.
- (46) Fong, H. H.; So, S. K. Hole Transporting Properties of Tris (8-Hydroxyquinoline) Aluminum (Alq3). *J. Appl. Phys.* **2006**, *100*, 094502–094502–5.
- (47) Van Mensfoort, S. L. M.; Shabro, V.; de Vries, R. J.; Janssen, R. A. J.; Coehoorn, R. Hole Transport in the Organic Small Molecule Material A-Npd: Evidence for the Presence of Correlated Disorder. *J. Appl. Phys.* **2010**, *107*, 113710–113710–8.
- (48) Rühle, V.; Junghans, C.; Lukyanov, A.; Kremer, K.; Andrienko, D. Versatile Object-Oriented Toolkit for Coarse-Graining Applications. *J. Chem. Theory Comput.* **2009**, *5*, 3211–3223.
- (49) Berendsen, H. J. C.; van der Spoel, D.; van Drunen, R. Gromacs: A Message-Passing Parallel Molecular Dynamics Implementation. *Comput. Phys. Commun.* **1995**, *91*, 43–56.
- (50) Ahlrichs, R.; Bär, M.; Häser, M.; Horn, H.; Kölmel, C. Electronic Structure Calculations on Workstation Computers: The Program System Turbomole. *Chem. Phys. Lett.* **1989**, *162*, 165–169.
- (51) Becke, A. D. A New Mixing of Hartree-Fock and Local Density-Functional Theories. *J. Chem. Phys.* **1993**, *98*, 1372–1377.
- (52) Schafer, A.; Horn, H.; Ahlrichs, R. Fully Optimized Contracted Gaussian Basis Sets for Atoms Li to Kr. *J. Chem. Phys.* **1992**, *97*, 2571–2577.
- (53) de Boer, B.; Hadipour, A.; Mandoc, M. M.; van Woudenberg, T.; Blom, P. W. Tuning of Metal Work Functions with Self-Assembled Monolayers. *Adv. Mater. (Weinheim, Ger.)* **2005**, *17*, 621–625.
- (54) Giordano, L.; Cinquini, F.; Pacchioni, G. Tuning the Surface Metal Work Function by Deposition of Ultrathin Oxide Films: Density Functional Calculations. *Phys. Rev. B* **2006**, *73*, 045414.
- (55) Coehoorn, R.; van Mensfoort, S. L. M. Effects of Disorder on the Current Density and Recombination Profile in Organic Light-Emitting Diodes. *Phys. Rev. B* **2009**, *80*, 085302.